Surgical Endoscopy
https://doi.org/10.1007/s00464-022-09304-9

Stapled fascial suture: ex vivo modeling and clinical implications

Enrico Lauro[1] · Ilaria Corridori[2,8] · Lorenzo Luciani[3] · Alberto Di Leo[4] · Alberto Sartori[5] · Jacopo Andreuccetti[6] · Diletta Trojan[7] · Giovanni Scudo[1] · Antonella Motta[8] · Nicola M. Pugno[2,9]

Received: 21 December 2021 / Accepted: 23 April 2022

Abstract

Background Recently, in the field of abdominal wall repair surgery, some minimally invasive procedures introduced the use of staplers to provide a retromuscular prosthetic repair. However, to the knowledge of the authors, there are little data in the literature about the outcomes of stapled sutures adoption for midline reconstruction. This study aims to investigate the biomechanics of stapled sutures, simple (stapled), or oversewn (hybrid), in comparison with handsewn suture. From the results obtained, we tried to draw indications for their use in a clinical context.

Methods Human cadaver fascia lata specimens, sutured (handsewn, stapled, or hybrid) or not, underwent tensile tests. The data on *strength* (maximal stress), *ultimate strain* (deformability), *Young's modulus* (rigidity), and *dissipated specific energy* (ability to absorb mechanical energy up to the breaking point) were recorded for each type of specimens and analyzed.

Results Stapled and hybrid suture showed a significantly higher *strength* (handsewn 0.83 MPa, stapled 2.10 MPa, hybrid 2.68 MPa) and a trend toward a lower *ultimate strain* as compared to manual sutures (handsewn 344%, stapled 249%, hybrid 280%). Stapled and hybrid sutures had fourfold higher *Young's modulus* as compared to handsewn sutures (handsewn 1.779 MPa, stapled 7.374 MPa, hybrid 6.964 MPa). Handsewn and hybrid sutures showed significantly higher *dissipated specific energy* (handsewn 0.99 mJ-mm^3, stapled 0.73 mJ-mm^3, hybrid 1.35 mJ-mm^3).

Conclusion Stapled sutures can resist high loads, but are less deformable and rigid than handsewn suture. This suggests a safer employment in case of small defects or diastasis (< W1 in accord to EHS classification), where the presumed tissutal displacement is minimal.

Oversewing a stapled suture improves its efficiency, becoming crucial in case of larger defects (> W1 in accord to EHS classification) where the expected tissutal displacement is maximal. Hybrid sutures seem to be a good compromise.

Keywords Diastasis recti · Stapled repair · Tensile test · Anterior rectus sheath plication · Laparo-endoscopic · Minimally invasive

In the field of abdominal wall repair surgery, the minimally invasive techniques are gaining an increasing interest. In

Enrico Lauro and Ilaria Corridori have contributed equally to this work.

✉ Enrico Lauro
enrico.lauro@apss.tn.it

✉ Nicola M. Pugno
nicola.pugno@unitn.it

[1] Department of General Surgery, St. Maria Del Carmine Hospital, Rovereto, Italy

[2] Laboratory for Bioinspired, Bionic, Nano, Meta Materials and Mechanics, Department of Civil, Environmental and Mechanical Engineering, University of Trento, Trento, Italy

[3] Robotic Unit and Department of Urology, Santa Chiara Hospital, Trento, Italy

[4] Department of General Surgery, San Camillo Hospital, Trento, Italy

[5] Department of General Surgery, Montebelluna-Castelfranco Veneto Hospital, Treviso, Italy

[6] Department of General Surgery 2^, ASST Spedali Civili di Brescia, Brescia, Italy

[7] Fondazione Banca dei Tessuti Treviso FBTV, Treviso, Italy

[8] Present Address: BIOtech Center for Biomedical Technologies, Department of Industrial Engineering, University of Trento, Trento, Italy

[9] School of Engineering and Material Science, Queen Mary University of London, London, UK

Published online: 16 May 2022

1993, LeBlanc first described laparoscopic hernia repair with the placement of an intraperitoneal mesh that provided a shorter length of hospital stay, less surgical site infection, and a recurrence rate similar to open techniques [1]. Afterward, to avoid the related risk of mesh adhesions with the abdominal viscera, which can lead to enteric fistulae, infections, and prosthesis displacement, several techniques have been developed to combine the advantages of minimally invasive surgery with the placement of a retromuscular mesh. Trans-abdominal preperitoneal approach (TAPP), totally endoscopic sublay repair (TES), endoscopic mini/less open sublay technique (EMILOS), retrorectal sublay mesh repair, and extended-view totally extraperitoneal approach (e-TEP) combine the advantages of laparoscopic surgery, with the consolidated results of the Rives–Stoppa repair, which is it still considered the gold standard in ventral hernia repair [2–8].

Recently, some minimally invasive procedures use staplers to provide a retromuscular prosthetic repair [9–13].

Staplers are widely used for gastrointestinal, vascular, and thoracic surgery [14–17].

The advantages of stapling include rapidity and reproducibility, the absence of knots, a homogeneous tension along the suture line, and the chance of employment in laparoendoscopic surgery [2].

On the other hand, it has been also reported that stapling failure can occur [18–23].

Oversewn stapled suture line appears to be correlated with lower complications rate, such as leakage and bleeding [24–27].

However, to the knowledge of the authors, there are a little data in the literature about the outcomes of stapled sutures adoption for midline reconstruction [28].

Even the clinical indications remain vague and are mainly based on the experience of each surgeon.

This study aims to investigate the biomechanics of stapled sutures, handsewn, or hybrid, on fascial aponeuroses, to understand their behavior under traction, their strengths, but above all their critical issues, trying to make these scientific data useful for technological improvements and in the clinical context.

Materials and methods

Design of the study and data collection

Fascia lata was harvested from human cadavers. Tensile tests were performed on four types of samples:

- Intact (unsutured) fascia lata (number of samples $n=5$);
- Fascia lata with handsewn suture ($n=5$);
- Fascia lata with stapled suture ($n=6$);
- Fascia lata with hybrid suture ($n=5$).

The primary outcomes were as follows:

1. To compare the mechanical properties of handsewn, stapled, and hybrid sutures.
2. To compare the mode of failure and the failure area of the different sutured samples.

The secondary outcomes were as follows:

1. To study whether the fiber orientation affects the tensile performance.
2. To compare the tensile behavior of unsutured fascia lata samples to sutured samples.

Features, collection, and processing of the fascia lata tissue

Cadaver fascia lata allografts were collected, processed, and cryopreserved by Treviso Tissue Bank Foundation (FBTV) following the requirements approved by the National Transplant Center. Donor selection includes serological tests for infectious diseases, and all tissues were decontaminated two times with a validated antibiotic cocktail [29].

Microbiological tests were performed following FBTV procedures. During the processing of fascia lata, adipose tissue and muscle tissue were removed. Tissues were stored at − 140 °C in liquid nitrogen vapor phase and thawed before their use.

The harvested patches were characterized by a fibrous structure embedded in a matrix, with an aligned or randomized orientation of the fibers. A digital caliper was used to measure the mean thickness of the patches [30]. The average thickness of the patches was 1.24 ± 0.29 mm. The samples were composed of two fascia lata halves of 4×4 cm sutured together, and samples of unsutured fascia lata measuring 8 cm × 4 cm. To test the sutures in physiological conditions, samples were released in a heated saline solution at 37 °C before testing [31].

Fascia lata samples and types of sutures

Three different types of sutures performed by one investigator were tested (Fig. 1):

- *Handsewn ($n=5$)*: Sutures were performed in a simple running pattern with polydioxanone (PDS II 2-0, Ethicon™). Tissue bites were placed every 5 mm from the wound edge, with inter-suture spacing of 5 mm (*small bites technique*) [32].

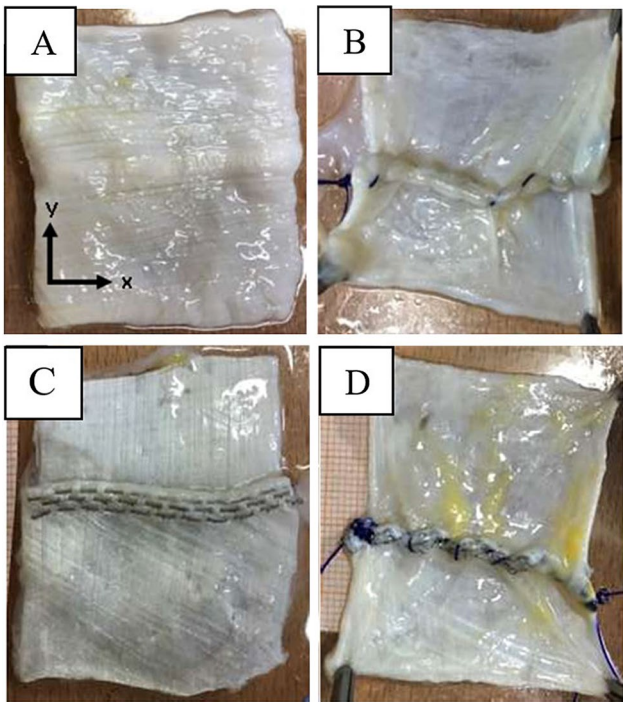

Fig. 1 **A** Intact fascia lata, (black arrows for x/y-fiber orientation); **B** handsewn suture; **C** stapled suture; **D** hybrid suture

- *Stapled (n = 6)*: A disposable endoscopic stapler was used to obtain a mechanical suture. Each suture is made of three rows of titanium staples with three different heights (Tri-Staple™ technology, Medtronic), respectively, of 3.0 mm, 3.5 mm, and 4.0 mm. The closed staples height ranges from 1.25 to 1.75 mm. Before firing across the fascial tissue, the two branches of the stapler were held in place for 15 seconds after closing and before firing, to ensure a better compression and staple formation.
- *Hybrid (n = 5)*: A stapled suture (Tri-Staple™ technology, Medtronic) was oversewn with a small bites running suture (PDS II 2-0, Ethicon™).

Tensile test

Tensile tests were performed with a Messphysik MIDI 10-20 Machine. A Mettler Toledo 500 N load cell was used with a tensile module. The tensile load was applied in quasi-static conditions, setting a 1 mm/s displacement speed. The total distance between the two grips was 2 cm (gauge length), and the suture was placed in the middle [Fig. 2A]. The sutures had different heights: 2.73 ± 0.48 mm in the handsewn, 2.64 ± 0.14 mm in the stapled, and 2.83 ± 0.33 mm in the hybrid suture. During tensile tests, the top patch was pulled vertically up to its breaking point (Fig. 2), and the tests were stopped when the complete breakage of the sample occurred.

Each test was recorded with a camera (SONY 4 K FDR-AX700). The first event causing a sudden decrease of the recorded force was considered as the failure.

Failure was classified according to the damaged area. The *junction failure* was defined as the slipping of one of the patches from the bordering edge, without breaking the rest of the tissue. *Tissue failure* is the breakage of the tissue distant from the suture. The area of failure was specified. The orientation of the fibers of each sample was investigated with the camera as *y*-oriented (parallel to the direction of the applied force), *x*-oriented (orthogonally to the direction of the applied force), or *randomly* oriented.

Stress (the force divided by the cross-sectional area)–strain (the displacement divided by the gauge length) curves were obtained to compare the different types of sutures and the unsutured samples. To obtain a more cautelative value of the stress, the rectangular cross-sectional area was calculated considering the thickest of the two sutured patches.

To evaluate the tensile behavior of the samples, four properties obtained from the stress–strain curves were considered:

(a) *Strength* (σ_f): The highest stress reached during the tensile test.
(b) *Ultimate strain* (ε_u): The ratio of length increment to initial length along the direction of stress at the break-

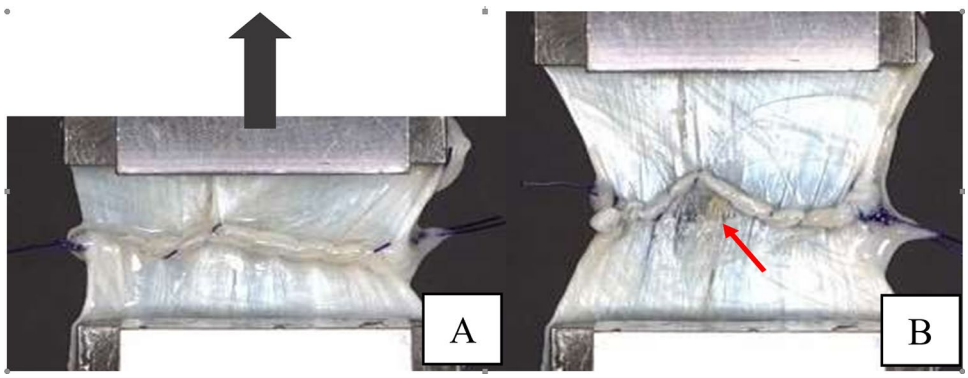

Fig. 2 Tensile test on a handsewn suture sample. **A** The arrow shows the direction of the applied tensile load. **B** The arrow underlines the failure event (pull-out of the suture) which led to the decrease of the force recorded

ing point; it defines the deformability of a material when a force is applied.

(c) *Young's modulus* (*E*): The longitudinal stress divided by the strain, as expressed by the slope in the first linear region of the stress/strain curve; it describes the elastic property of a solid undergoing lengthwise tension.

(d) *Dissipated specific energy* (*W*): The area under the stress–strain curve up to the ultimate strain (ε_u); it defines the ability to absorb mechanical energy up to the breaking point, also called toughness modulus.

Statistical analysis

The force and displacement values of each sample were measured with the tensile tests. The mechanical properties (strength, ultimate strain, Young's modulus, and dissipated specific energy) were calculated from the data obtained with the tensile tests. Subsequently, mean values and the standard deviations of each considered mechanical property were computed. Student's t test was performed to verify statistically significant differences ($p < 0.05$) between the mechanical properties of the three types of samples (handsewn, stapled, and hybrid suture).

Results

Data collected from samples with a different orientation of the fibers were heterogeneous and not comparable, in accordance with Henderson et al. [33]. Samples with fibers mainly oriented parallel to the suture line (*x*-oriented) showed a worse tensile performance compared to samples with *y*-oriented fibers. To reduce the influence of fiber orientation, only the results of stress–strain curves on *y*-oriented fibers (intact fascia lata $n = 3$; handsewn $n = 4$; stapled $n = 3$; hybrid $n = 3$) were considered (Fig. 3).

- *Strength*. Stapled and hybrid suture showed a higher strength as compared to handsewn sutures (handsewn 0.83 MPa, stapled 2.10 MPa, hybrid 2.68 MPa) with significant difference (handsewn vs stapled $p = 0.004$; handsewn vs. hybrid $p = 0.005$); hybrid sutures presented higher strength than stapled sutures, without statistically significant difference ($p = 0.31$).
- *Ultimate strain*. A trend toward a lower strain of stapled and hybrid sutures versus handsewn was found, although non-statistically significant (handsewn 344.91%, stapled 249.16%, hybrid 280.75%).
- *Young's modulus*. Stapled and hybrid sutures were about fourfold higher as compared to handsewn sutures (handsewn 1.779 MPa, stapled 7.374 MPa, hybrid 6.964 MPa) with statistically significant difference (handsewn vs stapled $p = 0.002$; handsewn vs. hybrid $p = 0.005$); sig-

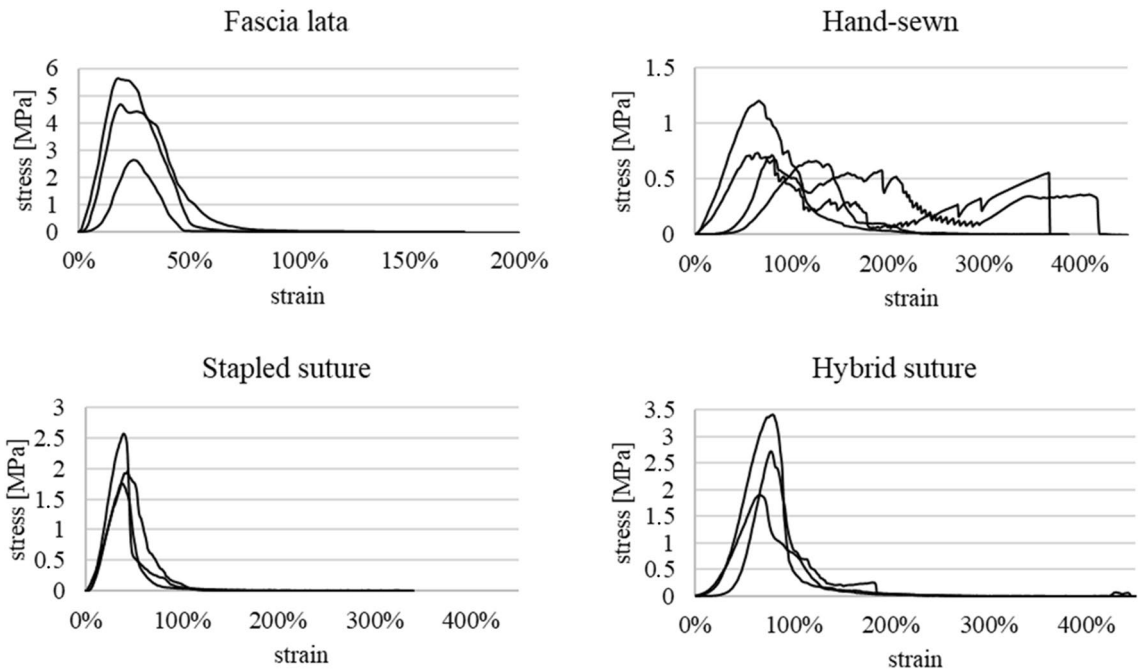

Fig. 3 Tensile test curves on samples with y-oriented fibers

nificant difference was not observed between stapled and hybrid sutures ($p = 0.82$).

- *Dissipated specific energy*. Handsewn and hybrid sutures showed higher values as compared to stapled sutures (handsewn 0.99 mJ·mm^{-3}, vs. stapled 0.73 mJ·mm^{-3}, vs. hybrid 1.35 mJ·mm^{-3}), with a significant difference between stapled and hybrid sutures ($p = 0.02$).

The mean values of the calculated mechanical properties obtained with the three types of sutures are presented in Fig. 4.

Mode of failure and failure area

All the tested samples broke due to junction failure. A different area of failure was observed according to the different sutures. The handsewn-sutured samples broke at the end knots. In the stapled-sutured samples, the patches were uniformly pulled out along the suture line in two of three cases; the hybrid suture failed both at the end knots (two cases) and with the complete breakage of the patch due to its pull-out in one case.

Unsutured fascia lata

The highest mechanical properties were recorded on samples with *y*-directed fibers (strength 4.32 MPa, Young's modulus 32.33 MPa, dissipated specific energy 1.26 mJ/mm^3), except the ultimate strain which was higher in the samples composed of randomly oriented fibers (570.81%). During the tests on samples with fibers parallel to the tensile direction (*y*-oriented) the top grip of the tensile machine slipped from the specimen.

Discussion and conclusion

Stapled closure of fascial tissues has been recently adopted for laparo-endoscopic midline repair [9–13], but their use is controversial since their advantages (i.e., rapidity and

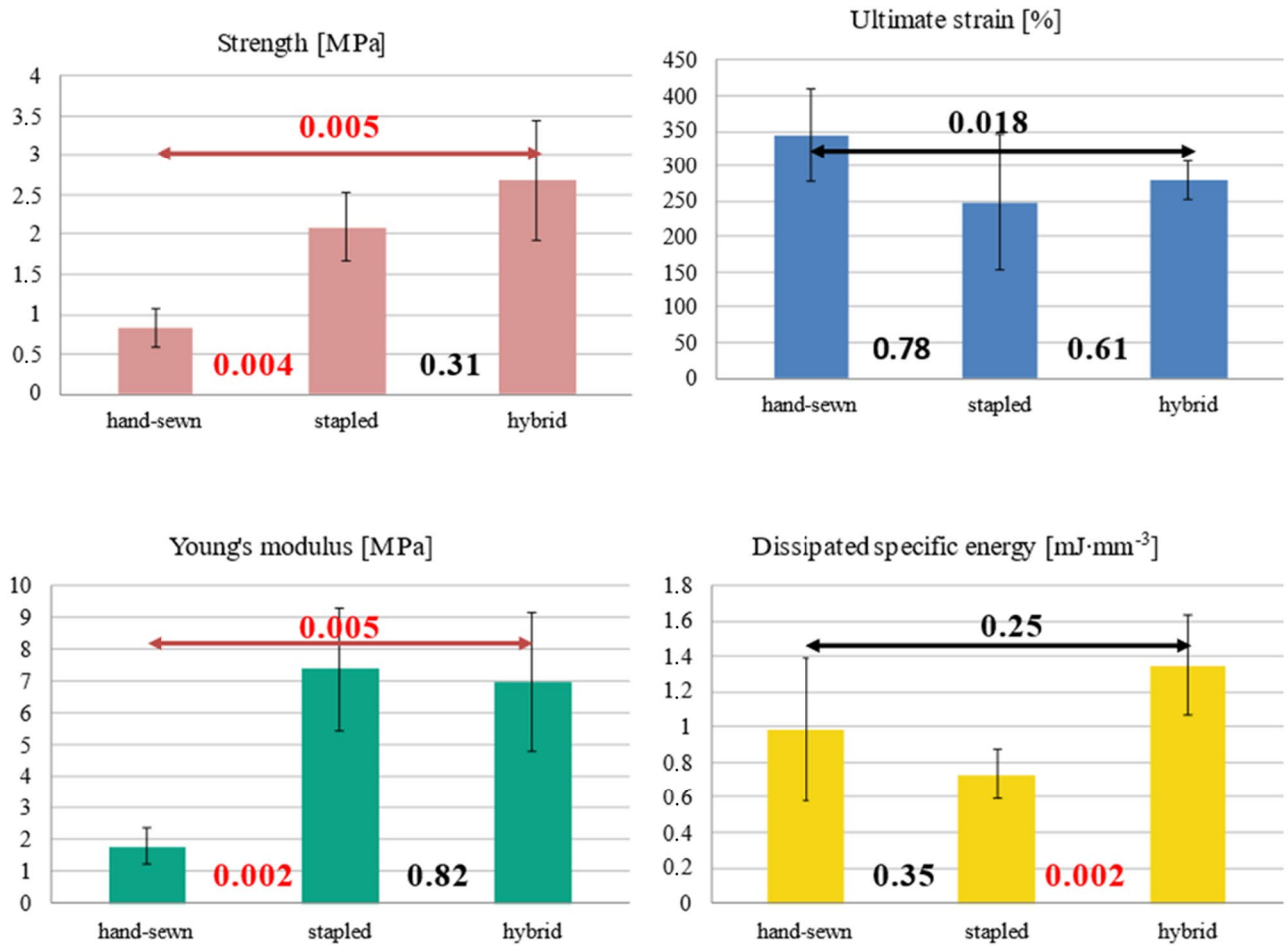

Fig. 4 Comparison between mechanical properties of handsewn, stapled, and hybrid sutures

reproducibility, absence of knots, homogeneous tension along the suture) are obscured by a lack of evidence in the literature.

Staplers are employed to join the posterior and anterior rectus sheaths together, developing the retromuscular space for mesh reinforcement (Fig. 5).

The novelty introduced is a purely technological aspect, represented by the synthesis of the anterior and posterior fascial layers through a mechanical device.

As in other fields of general surgery, where oversewn the staple suture appears to be correlated with lower complications rate, such as leakage or bleeding [24–27], the stapled suture can be manually reinforced, either to improve its tensile resistance and to increase the plication of the rectus muscles during diastasis repair (Fig. 5D).

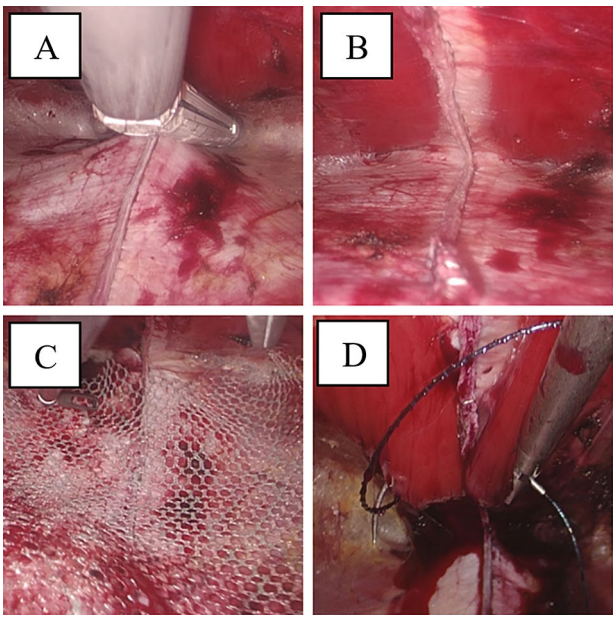

Fig. 5 **A** Endo stapler firing (during surgical operation by an author); **B** retromuscular space development; **C** sublay mesh reinforcement; **D** stapled suture oversewn

The higher stiffness and less vascularisation of fascial tissues as compared to other organs may further limit their use in this context [34, 35].

Furthermore, any type of suture on muscle-aponeurotic structures must resist higher forces than on other tissues [34] (e.g., bowel, vessels, or bronchus).

The stapled suture may fail due to opening of the row of staples, with possible formation of an internal hernia (Fig. 6A) or breakage of the fascial tissue along the suture line, with consequent prosthetic exposure into the abdominal cavity (Fig. 6B).

Nowadays, no data on the biomechanical properties of stapled sutures on human fasciae are available, and their use is often based on useful anecdotal experience as surgeons, without achieving the necessary mandatory level of objective evidence by studying their mechanical properties.

Tensile tests on cadaveric fascia lata specimens were performed due to their similarities with the aponeurotic sheaths of the rectus abdominis muscle.

Directly testing linea alba samples, instead of fascia lata, would not have had a greater methodological value, because in case of hernias or diastasis the midline is absent, replaced by scar tissue or deeply altered.

Furthermore, restoring the linea alba and its anatomic 3D characteristics through a surgical repair is not possible, because the neo-midline will be composed by scar tissue, with less resistance to multidirectional stresses and very different from its original structure.

Different types of mechanical testing (e.g., tensile tests, cyclic tests, fatigue tests, dynamic intermittent strain test [36–39]) should be performed to obtain a comprehensive description of the biomechanics of the studied tissue/material. The data should be consequently linked and correlated

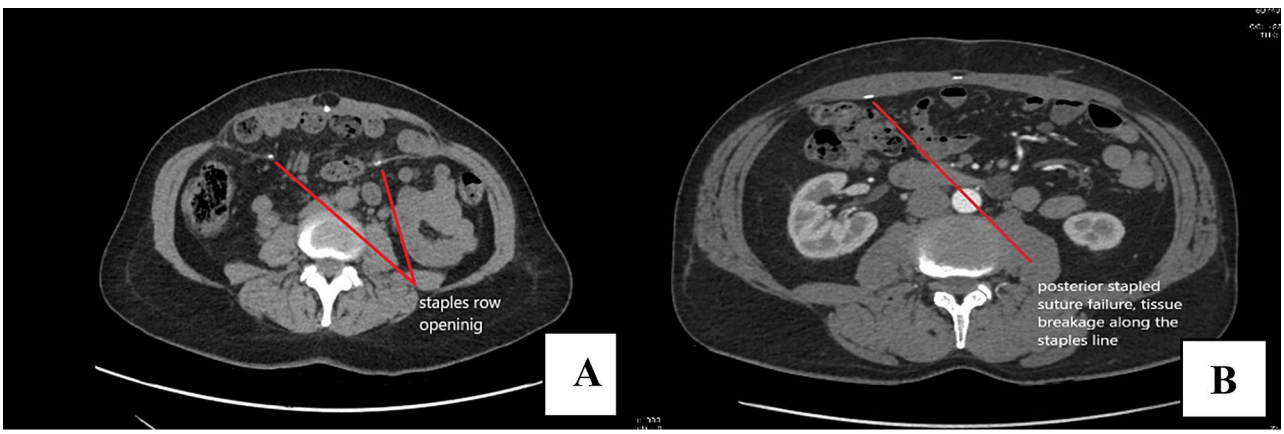

Fig. 6 **A** Posterior staples row opening and "internal" hernia formation (as observed by us); **B** posterior stapled suture failure for tissue breakage along the suture line: intraperitoneal mesh exposure

to have a complete description of the interaction between host tissue, mesh, and fixation devices.

To obtain reliable results, potentially capable of describing the physiological conditions of living tissues, we performed mechanical tests immediately after removing the samples from the heated saline solution at 37 °C as previously described by other authors [33].

The tensile tests lasted 50 s on average and the samples resulted hydrated.

Furthermore, we used human fascia lata samples, similar to the rectus sheaths and already used in ventral hernia surgery [40–44].

Primary endpoints

Tensile tests on sutured samples

This study suggests that stapled and hybrid sutures have better rigidity (Young's modulus) and strength performances than handsewn sutures, implying that stapled sutures, alone or oversewn, can resist high tensile forces per cross-sectional tissue area. Indeed, the absence of knots and a balanced load along the staplers' rows make stapled sutures more stable as compared to handsewn sutures [2, 35].

However, stapled and hybrid sutures have lower ultimate strain values, showing less deformability than handsewn sutures.

Thus, less efficiency is expected for mechanical sutures in case of high tissue displacements or when a more deformable behavior is needed as in case of large midline defects closure (e.g., W2 in accord to EHS classification).

Handsewn sutures, both handsewn and oversewn, absorb higher mechanical energy up to the breaking point, thus assuming characteristics more similar to intact and non-sutured tissue, whereas stapled sutures showed to be less tough.

An hybrid suture, as compared to a stapled suture, gains in terms of overall strength, ultimate strain, Young's modulus, and dissipated specific energy, suggesting the need for hybrid sutures in case of larger fascial defects or higher tension expected along the suture line.

Mode of failure and failure area

In handsewn sutures, end knots represent an area of weakness under tensile stress [45].

Stapled sutures show a uniform failure mode along the suture line, where the load is equally distributed without different weakness zones. Each entry bite of the staples represents itself a single weakness area, one equal to the other, and uniformly distributed along the suture, where the force lines act up to the breaking point in an "all or nothing" model.

Hybrid sutures show an intermediate failure behavior between handsewn and stapled sutures, probably due to interaction between handsewn and stapled sutures in the breaking event.

Secondary endpoints

Fibers orientation

The secondary endpoint investigated shows that fibers orientation with respect to the applied force influences the tensile performance of the sutures. Thus, comparing samples with different fibers orientation was not possible, as reported by previous investigators [33, 36]. Fasciae with fibers oriented parallel the applied force show better results in terms of overall stress, ultimate strain, Young's modulus, and dissipated specific energy.

Intact vs. sutured fascia lata

Results show that intact samples of fascia lata present higher resistance (4.32 MPa). Comparing these data to the results obtained with sutured samples, it is possible to conclude that a suture nearly halves (stapled 2.09 MPa and hybrid 2.68 MPa) or decreases fivefold (handsewn, 0.83 MPa) the strength of the tissue when loaded with a tensile force.

Drawing clinical indications from an ex vivo model will always be debated, but at the same time we are encouraged from previous studies demonstrating the potential to be useful for adoption of surgical novelties [46, 47].

The advantage of this model is the chance to control single variables (tissue thickness, staples height, stapling technique, handsewn suture technique) affecting the expected results.

The small sample size and the difficulty to apply the experimental results to surgical practice are the limitations of our study.

Moreover, the rectus sheath and linea alba fibers are anisotropic [34] and distributed to resist multidirectional forces, as opposed to the unidirectional force applied in experimental conditions.

However, the experiments were conducted in a standardized fashion obtaining consistent results for each type of suture.

In conclusion, the ideal suture should be resistant to high loads (strength), high deformable (ultimate strain), and stiff (Young's modulus), able to absorb high energy (toughness).

These properties are not yet available in only one suture, and choosing which one to use should be a balance between pros and cons.

Stapled sutures can resist high loads but, by contrast, are less deformable than handsewn sutures.

This suggests a safer employment in case of small defects or diastasis (< W1 in accord to EHS classification), where the presumed tissue displacement is minimal.

Oversewing a stapled suture improves its deformability, becoming crucial in case of larger defects (> W1 in accord to EHS classification) where the presumed tissue displacement is maximal (e.g., in stout male patients, thick lateral muscles, elevated BMI).

A careful preoperative patient assessment (patient selection, imaging, preoperative botulin toxin A injection) coupled with intraoperative precautions (correct stapling technique, right staples height choice, oversewn reinforcement) can be helpful in controlling intra- and post-operative complications, such as staples opening, suture failure, intraperitoneal mesh exposure, and recurrences.

Further larger studies, including in vivo models, will be needed to confirm our results and to pave the way to develop staplers dedicated to this type of surgery.

Supplementary Information The online version contains supplementary material available at https://doi.org/10.1007/s00464-022-09304-9.

Acknowledgements The authors thank the University of Trento and the San Camillo Hospital of Trento for their support. The authors also thank the Treviso Tissue Bank Foundation (FBTV) for providing the anatomic specimens. Special thanks to Prof. Davide Lomanto of the National University of Singapore for his valuable advice.

Author contributions The corresponding authors confirm that each author named in the by-line qualify by having participated actively and sufficiently in the study.

Funding No funding was received for this study.

Declarations

Disclosures Enrico Lauro, Ilaria Corridori, Lorenzo Luciani, Alberto Di Leo, Alberto Sartori, Jacopo Andreuccetti, Diletta Trojan, Giovanni Scudo, Antonella Motta, and Nicola M. Pugno have no conflict of interest or financial ties to disclose.

References

1. LeBlanc KA, Booth WV (1993) Laparoscopic repair of incisional abdominal hernias using expanded polytetrafluoroethylene: preliminary findings. Surg Laparosc Endosc 3:39–41
2. Bittner R, Bain K, Bansal VK, Berrevoet F, Bingener-Casey J, Chen D, Chen J, Chowbey P, Dietz UA, de Beaux A, Ferzli G, Fortelny R, Hoffmann H, Iskander M, Ji Z, Jorgensen LN, Khullar R, Kirchhoff P, Köckerling F, Kukleta J, LeBlanc K, Li J, Lomanto D, Mayer F, Meytes V, Misra M, Morales-Conde S, Niebuhr H, Radvinsky D, Ramshaw B, Ranev D, Reinpold W, Sharma A, Schrittwieser R, Stechemesser B, Sutedja B, Tang J, Warren J, Weyhe D, Wiegering A, Woeste G, Yao Q (2019) Update of Guidelines for laparoscopic treatment of ventral and incisional abdominal wall hernias (International Endohernia Society (IEHS))—Part A. Surg Endosc 33:3069–3139. https://doi.org/10.1007/S00464-019-06907-7/FIGURES/4
3. Claus CMP, Malcher F, Cavazzola LT, Furtado M, Morrell A, Azevedo M, Meirelles LG, Santos H, Garcia R (2018) Subcutaneous onlay laparoscopic approach (SCOLA) for ventral hernia and rectus abdominis diastasis repair: technical description and initial results. Arq Bras Cir Dig 31:1–5. https://doi.org/10.1590/0102-672020180001e1399
4. Chowbey PK, Sharma A, Khullar R, Soni V, Baijal M (2003) Laparoscopic ventral hernia repair with extraperitoneal mesh: surgical technique and early results. Surg Laparosc Endosc Percutaneous Tech 13:101–105. https://doi.org/10.1097/00129689-200304000-00008
5. Schwarz J, Reinpold W, Bittner R (2017) Endoscopic mini/less open sublay technique (EMILOS)-a new technique for ventral hernia repair. Langenbeck's Arch Surg 402:173–180. https://doi.org/10.1007/s00423-016-1522-0
6. Jani K, Contractor S (2019) Retrorectus sublay mesh repair using polypropylene mesh: Cost-effective approach for laparoscopic treatment of ventral abdominal wall hernias. J Min Access Surg 15:287–292. https://doi.org/10.4103/jmas.JMAS_20_19
7. Li B, Qin C, Bittner R (2018) Totally endoscopic sublay (TES) repair for midline ventral hernia: surgical technique and preliminary results. Surg Endosc 34(4):1543–1550. https://doi.org/10.1007/S00464-018-6568-3
8. Andreuccetti J, Sartori A, Lauro E, Crepaz L, Sanna S, Pignata G, Bracale U, di Leo A (2021) Extended totally extraperitoneal rives-stoppa (eTEP-RS) technique for ventral hernia: initial experience of The Wall Hernia Group and a surgical technique update. Updates Surg 73(5):1955–1961. https://doi.org/10.1007/S13304-021-01067-7
9. Abdalla RZ, Garcia RB, da Costa RID, Abdalla BMZ (2013) Treatment of mid-line abdominal wall hernias with the use of endo-stapler for mid-line closure. Arq Bras Cir Dig 26:335–337. https://doi.org/10.1590/S0102-67202013000400016
10. Costa TN, Abdalla RZ, Santo MA, Tavares RRFM, Abdalla BMZ, Cecconello I (2016) Transabdominal midline reconstruction by minimally invasive surgery: technique and results. Hernia 20(2):257–265. https://doi.org/10.1007/S10029-016-1457-Y
11. Moore AM, Anderson LN, Chen DC (2016) Laparoscopic stapled sublay repair with self-gripping mesh: a simplified technique for minimally invasive extraperitoneal ventral hernia repair. Surg Technol Int 29:131–139
12. Nguyen DK, Chen DC (2017) Laparoendoscopic stapled rives stoppa sublay technique for extraperitoneal ventral hernia repair. Eur Surg 49:175–179. https://doi.org/10.1007/S10353-017-0483-Z
13. Carrara A, Lauro E, Fabris L, Frisini M, Rizzo S (2019) Endolaparoscopic reconstruction of the abdominal wall midline with linear stapler, the THT technique. Early results of the first case series. Ann Med Surg 38:1–7. https://doi.org/10.1016/J.AMSU.2018.12.002
14. Maeda K, Maruta M, Utsumi T, Sato H, Masumori K, Matsumoto M (2002) Minimally invasive surgery for carcinoid tumors in the rectum. Biomed Pharmacother 56(Suppl 1):222s–226s. https://doi.org/10.1016/s0753-3322(02)00218-4
15. Tejedor P, Sagias F, Nock D, Flashman K, Naqvi S, Kandala NL, Khan JS (2019) Advantages of using a robotic stapler in rectal cancer surgery. J Robot Surg 14(2):365–370. https://doi.org/10.1007/S11701-019-00993-4
16. Roberts KE, Renee Hilton L, Friedman DT, Frieder JS, Zhang X, Duffy AJ (2018) Safety and feasibility of a lower-cost stapler in bariatric surgery. Obes Surg 29(2):401–405. https://doi.org/10.1007/S11695-018-3580-6

17. Müller-Stich B, Schmidt T, Nienhüser H, Nickel F, Billeter A, Diener M, Ulrich A, Büchler MW (2020) Total-minimalinvasive Ösophagektomie. Chirurg 91(1):13–14. https://doi.org/10.1007/S00104-020-01152-4
18. Makanyengo SO, Thiruchelvam D (2020) Literature review on the incidence of primary stapler malfunction. Surg Innov 27:229–234. https://doi.org/10.1177/1553350619889274
19. Gossot D, Merlusca G, Tudor A, Boudaya MS, Radu C, Magdeleinat P (2008) Pitfalls related to the use of endostaplers during video-assisted thoracic surgery. Surg Endosc 23(1):189–192. https://doi.org/10.1007/S00464-008-9765-7
20. Yano M, Yokoi K, Numanami H, Kondo R, Ohde Y, Sugaya M, Narita K, Chihara K, Matsushima Y, Kobayashi R, Hikosaka Y (2013) Complications of bronchial stapling in thoracic surgery. World J Surg 38(2):341–346. https://doi.org/10.1007/S00268-013-2292-2
21. Major P, Wysocki M, Pędziwiatr M, Pisarska M, Małczak P, Wierdak M, Dembiński M, Migaczewski M, Rubinkiewicz M, Budzyński A (2018) More stapler firings increase the risk of perioperative morbidity after laparoscopic sleeve gastrectomy. Videosurg Other Miniinvasive Tech 13:88–94. https://doi.org/10.5114/wiitm.2017.70197
22. Lundvall E, Ottosson J, Stenberg E (2019) The influence of staple height on postoperative complication rates after laparoscopic gastric bypass surgery using linear staplers. Surg Obes Relat Dis 15:404–408. https://doi.org/10.1016/J.SOARD.2019.01.017
23. Nordholm-Carstensen A, Rasmussen MS, Krarup PM (2019) Increased leak rates following stapled versus handsewn ileocolic anastomosis in patients with right-sided colon cancer: a nationwide cohort study. Dis Colon Rectum 62:542–548. https://doi.org/10.1097/DCR.0000000000001289
24. Lin S, Li C, Guan W, Liang H (2021) Can staple-line reinforcement eliminate the major early postoperative complications after sleeve gastrectomy? Asian J Surg 44:836–840. https://doi.org/10.1016/j.asjsur.2020.12.036
25. Baqar AR, Wilkins S, Staples M, Oliva K, McMurrick P (2020) The post-operative impact of oversewing stapled anastomoses in colorectal cancer surgery: a retrospective Australian cohort study. Int J Surg Open 24:91–95. https://doi.org/10.1016/j.ijso.2020.04.004
26. Demeusy A, Sill A, Averbach A (2018) Current role of staple line reinforcement in 30-day outcomes of primary laparoscopic sleeve gastrectomy: an analysis of MBSAQIP data, 2015–2016 PUF. Surg Obes Relat Dis 14:1454–1461. https://doi.org/10.1016/J.SOARD.2018.06.024
27. Yo LSF, Consten ECJ, Quarles Van Ufford HME, Gooszen HG, Gagner M (2007) Buttressing of the staple line in gastrointestinal anastomoses: overview of new technology designed to reduce perioperative complications. Dig Surg 23:283–291
28. Carrara A, Catarci M, Fabris L, Zuolo M, Pellecchia L, Moscatelli P, Dorna A, Motter M, Pertile R, Tirone G (2021) Prospective observational study of abdominal wall reconstruction with THT technique in primary midline defects with diastasis recti: clinical and functional outcomes in 110 consecutive patients. Surg Endosc 35:5104–5114. https://doi.org/10.1007/s00464-020-07997-4
29. Paolin A, Spagnol L, Battistella G, Trojan D (2018) Evaluation of allograft decontamination with two different antibiotic cocktails at the treviso tissue bank foundation. PLoS ONE. https://doi.org/10.1371/journal.pone.0201792
30. Otsuka S, Yakura T, Ohmichi Y, Ohmichi M, Naito M, Nakano T, Kawakami Y (2018) Site specificity of mechanical and structural properties of human fascia lata and their gender differences: a cadaveric study. J Biomech 77:69–75. https://doi.org/10.1016/j.jbiomech.2018.06.018
31. Gras LL, Laporte S, Mitton D, Crevier-Denoix N, Viot P (2012) Tensile tests on a muscle: influence of experimental conditions and of velocity on its passive response. In: 2012 IRCOBI Conference Location: Dublin, Ireland. https://trid.trb.org/view/1254086. Accessed 7 Mar 2022
32. Israelsson LA (2015) Abdominal incision closure: small but important bites. Lancet 386:1216–1218. https://doi.org/10.1016/S0140-6736(15)60687-0
33. Henderson ER, Friend EJ, Toscano MJ, Parsons KJ, Tarlton JF (2015) Biomechanical comparison of canine fascia lata and thoracolumbar fascia: an in vitro evaluation of replacement tissues for body wall reconstruction. Vet Surg 44:126–134. https://doi.org/10.1111/J.1532-950X.2014.12247.X
34. Deeken CR, Lake SP (2017) Mechanical properties of the abdominal wall and biomaterials utilized for hernia repair. J Mech Behav Biomed Mater 74:411–427
35. Okami J, Tokunaga T, Kanou T, Kunou H, Ishida D, Fujiwara A, Ito Y, Higashiyama M (2017) Randomized study comparing equal height staples with graduated height staples in bronchial closure. Ann Thorac Surg 104:1012–1019. https://doi.org/10.1016/j.athoracsur.2017.02.070
36. Shimizu N, Tarlton J, Friend E, Doran I, Parsons K (2017) Tensile comparison of polydioxanone, polyglyconate, and barbed glycolide-trimethylene carbonate suture in canine cadaveric tensor fascia lata. Vet Surg 46:89–94. https://doi.org/10.1111/VSU.12580
37. Barber FA, Coons DA, Ruiz-Suarez M (2008) Cyclic load testing and ultimate failure strength of biodegradable glenoid anchors. Arthroscopy 24:224–228. https://doi.org/10.1016/J.ARTHRO.2007.08.011
38. Kallinowski F, Ludwig Y, Löffler T, Vollmer M, Lösel PD, Voß S, Görich J, Heuveline V, Nessel R (2021) Biomechanics applied to incisional hernia repair—considering the critical and the gained resistance towards impacts related to pressure. Clin Biomech. https://doi.org/10.1016/j.clinbiomech.2020.105253
39. Kallinowski F, Gutjahr D, Harder F, Sabagh M, Ludwig Y, Lozanovski VJ, Löffler T, Rinn J, Görich J, Grimm A, Vollmer M, Nessel R (2021) The grip concept of incisional hernia repair—dynamic bench test, CT Abdomen with Valsalva and 1-year clinical results. Front Surg. https://doi.org/10.3389/fsurg.2021.602181
40. Sekine Y, Sugo H, Iwanaga N, Neshime S, Watanobe I (2020) Relaparotomy two years after incisional hernia repair using a free fascia lata graft. Case Rep Surg 2020:1–4. https://doi.org/10.1155/2020/1769404
41. Morse LJ, Barb JS (1943) Free autoplastic transplants of fascia lata in the repair of large incisional hernia. Surgery 13:524–534. https://doi.org/10.5555/URI:PII:S0039606043903691
42. Goto A, Matsuhashi N, Takahashi T, Tanahashi T, Matsui S, Imai H, Tanaka Y, Yamaguchi K, Yoshida K (2020) Feasibility of the reconstruction with fascia lata patch on the abdominal wall defect after resection of the abdominal desmoid tumor. Clin Exp Gastroenterol 13:249–254. https://doi.org/10.2147/CEG.S249870
43. Sugo H, Kawai M, Miyano S, Watanobe I, Machida M, Kitabatake T, Lee Y, Kojima K (2019) Surgical repair with free fascia lata graft in patients at risk of surgical site infection: a case series. Int Surg 104:69–74. https://doi.org/10.9738/INTSURG-D-17-00053.1
44. Miyamoto Y, Watanabe M, Ishimoto T, Baba Y, Iwagami S, Sakamoto Y, Yoshida N, Masuguchi S, Ihn H, Baba H (2015) Fascia lata onlay patch for repairing infected incisional hernias. Surg Today 45:121–124. https://doi.org/10.1007/s00595-014-0936-y
45. Kim JC, Lee YK, Lim BS, Rhee SH, Yang HC (2007) Comparison of tensile and knot security properties of surgical

sutures. J Mater Sci 18:2363–2369. https://doi.org/10.1007/s10856-007-3114-6
46. Kerr AS, Osende J, Fallon JT, Badimon J (2001) Aortic slim-graft: ex vivo and in vivo study. J Vasc Surg 34:350–352. https://doi.org/10.1067/MVA.2001.115814
47. Patterson T, Witberg G, Redwood S, Prendergast B (2019) Balloon valve fracture at the time of valve-in-valve transcatheter aortic valve replacement: ex vivo modeling and clinical implications. JACC 12:76–77. https://doi.org/10.1016/J.JCIN.2018.11.021

STAPLED FASCIAL SUTURE: EX VIVO MODELING AND CLINICAL IMPLICATIONS

Enrico Lauro [1]§, Ilaria Corridori [2]*, Lorenzo Luciani [3], Alberto Di Leo [4], Alberto Sartori [5], Jacopo Andreuccetti [6], Diletta Trojan [7], Giovanni Scudo [1], Antonella Motta [8], Nicola M. Pugno [2,9]§*

[1] Department of General Surgery, St. Maria Del Carmine Hospital, Corso Verona 4, 38068 Rovereto, Italy. Email: enrico.lauro@apss.tn.it

[2] Laboratory for Bioinspired, Bionic, Nano, Meta Materials & Mechanics, Department of Civil, Environmental and Mechanical Engineering, University of Trento, Trento, Italy

[3] Robotic Unit and Department of Urology, Santa Chiara Hospital, Trento, Italy

[4] Department of General Surgery, San Camillo Hospital, Trento, Italy

[5] Department of General Surgery, Montebelluna-Castelfranco Veneto Hospital, Treviso, Italy

[6] Department of General Surgery 2^, ASST Spedali Civili di Brescia, Brescia, Italy

[7] Fondazione Banca dei Tessuti Treviso FBTV, Treviso, Italy

[8] Biotech Research Center, Department of Industrial Engineering, University of Trento, Italy

[9] School of Engineering and Material Science, Queen Mary University of London, London, United Kingdom

Supplementary Informations.

Tensile tests

Manual suture

Table S1 Mechanical properties of two fascia lata patches sutured with manual suture. One patch has x-oriented fibres and the other randomly oriented fibres. "t bottom" is the thickness of the patch attached to the bottom grip, "t top" is the thickness of the patch attached to the top grip, "fibres top" and "fibres bottom" are the orientation of the fibres of the bottom and top patch, "failure mode" and "failure area" are the event that led to a decrease of the force recorded and the area in which occurred. To quantify the tensile behaviour of the samples, four properties extracted from the stress-strain curves were considered: the strength (σ_f), the ultimate strain (ε_u), the Young's Modulus (E), and the dissipated specific energy (W) up to the sample complete failure.

#	sample	t bottom	t top	t tot suture	fibres bottom	fibres top	failure mode	failure area	σ_f [MPa]	ε_u [%]	E [MPa]	W [mJ·mm^{-3}]
1	manual suture	1.1	1.42	2.52	x	random	tissue failure	below the suture, middle bottom patch	0.62	303.59	1.48	0.37
3	manual suture	1.5	0.92	2.42	x	random	tissue failure	below the suture, middle	0.47	315.20	0.88	0.40

	bottom patch				
	mean	**0.54**	**309.40**	**1.18**	**0.39**
	st.dev.	**0.10**	**8.21**	**0.43**	**0.02**

Table S2 Mechanical properties of two fascia lata patches sutured with manual suture. The patches have y-oriented fibres. "t bottom" is the thickness of the patch attached to the bottom grip, "t top" is the thickness of the patch attached to the top grip, "fibres top" and "fibres bottom" are the orientation of the fibres of the bottom and top patch, "failure mode" and "failure area" are the event that led to a decrease of the force recorded and the area in which occurred. To quantify the tensile behaviour of the samples, four properties extracted from the stress-strain curves were considered: the strength (σ_f), the ultimate strain (ε_u), the Young's Modulus (E), and the dissipated specific energy (W) up to the sample complete failure.

#	sample	t bottom	t top	t tot suture	fibres bottom	fibres top	failure mode	failure area	σ_f [MPa]	ε_u [%]	E [MPa]	W [mJ·mm^{-3}]
4	manual suture	1.5	1.64	3.14	y	y	junction failure	bottom patch, middle right	0.71	368.29	1.94	0.96
5	manual suture	1	1.04	2.04	y	y	junction failure	top patch, middle left	1.21	289.39	2.44	0.92
6	manual suture	1.56	1.44	3	y	y	junction failure	top patch, right and left ends	0.66	294.18	1.14	0.54
7	manual suture	1.74	0.99	2.73	y	y	junction failure	bottom patch, middle left	0.73	427.78	1.60	1.52
								mean	**0.83**	**344.91**	**1.78**	**0.99**
								st.dev.	**0.25**	**66.01**	**0.55**	**0.41**

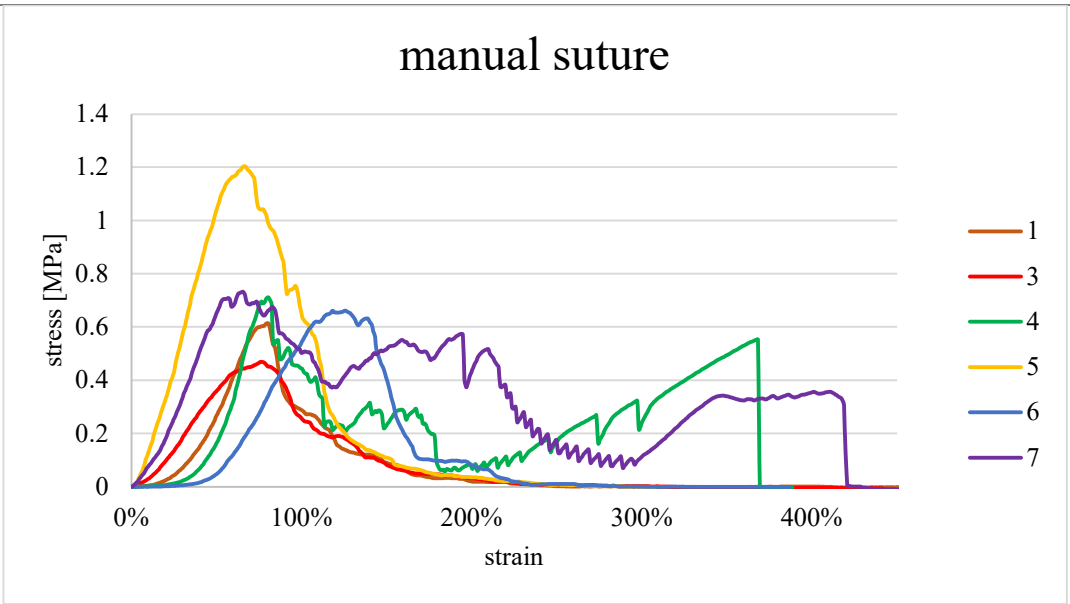

Figure S1 Stress-strain curves obtained with tensile tests on fascia lata patches with handsewn (manual) suture. The legend shows the name of the samples ("#" in the tables).

Stapled sutures

Table S3 Mechanical properties of two fascia lata patches sutured with stapled suture. One patch has x-oriented fibres and the other y-oriented fibres."t bottom" is the thickness of the patch attached to the bottom grip, "t top" is the thickness of the patch attached to the top grip, "fibres top" and "fibres bottom" are the orientation of the fibres of the bottom and top patch, "failure mode" and "failure area" are the event that led to a decrease of the force recorded and the area in which occurred. To quantify the tensile behaviour of the samples, four properties extracted from the stress-strain curves were considered: the strength (σ_f), the ultimate strain (ε_u), the Young's Modulus (E), and the dissipated specific energy (W) up to the sample complete failure.

#	sample	t bottom	t top	t tot suture	fibres bottom	fibres top	failure mode	failure area	σ_f [MPa]	ε_u [%]	E [MPa]	W [mJ·mm^{-3}]
4	stapled suture	1.09	0.93	2.02	y	x	tissue failure	middle left top patch	0.856	424.6	4.747	0.50
5	stapled suture	1.5	1.16	2.66	x	y	tissue failure	left bottom patch	0.607	465.29	2.192	0.33
6	stapled suture	1.35	1.56	2.91	y	x	tissue failure	middle top patch	1.231	153.99	4.256	0.40
								mean	**0.90**	**347.96**	**3.73**	**0.41**
								st.dev.	**0.31**	**169.21**	**1.36**	**0.08**

Table S4 Mechanical properties of two fascia lata patches sutured with stapled suture. The patches have y-oriented fibres."t bottom" is the thickness of the patch attached to the bottom grip, "t top" is the thickness of the patch attached to the top grip, "fibres top" and "fibres bottom" are the orientation of the fibres of the bottom and top patch, "failure mode" and "failure area" are the event that led to a decrease of the force recorded and the area in which occurred. To quantify the tensile behaviour of the samples, four properties extracted from the stress-strain curves were considered: the strength (σ_f), the ultimate strain (ε_u), the Young's Modulus (E), and the dissipated specific energy (W) up to the sample complete failure.

#	sample	t bottom	t top	t tot suture	fibres bottom	fibres top	failure mode	failure area	σ_f [MPa]	ε_u [%]	E [MPa]	W [mJ·mm^{-3}]
1	stapled suture	1.15	1.43	2.58	y	y	junction failure	total top patch	1.76	329.40	6.83	0.57
2	stapled suture	1.09	0.81	1.90	y	y	junction failure	total top patch	2.58	276.79	9.52	0.78
3	stapled suture	1.39	0.98	2.37	y	y	junction failure	half top patch	1.96	141.28	5.77	0.85
								mean	**2.10**	**249.16**	**7.37**	**0.73**
								st.dev.	**0.43**	**97.06**	**1.93**	**0.14**

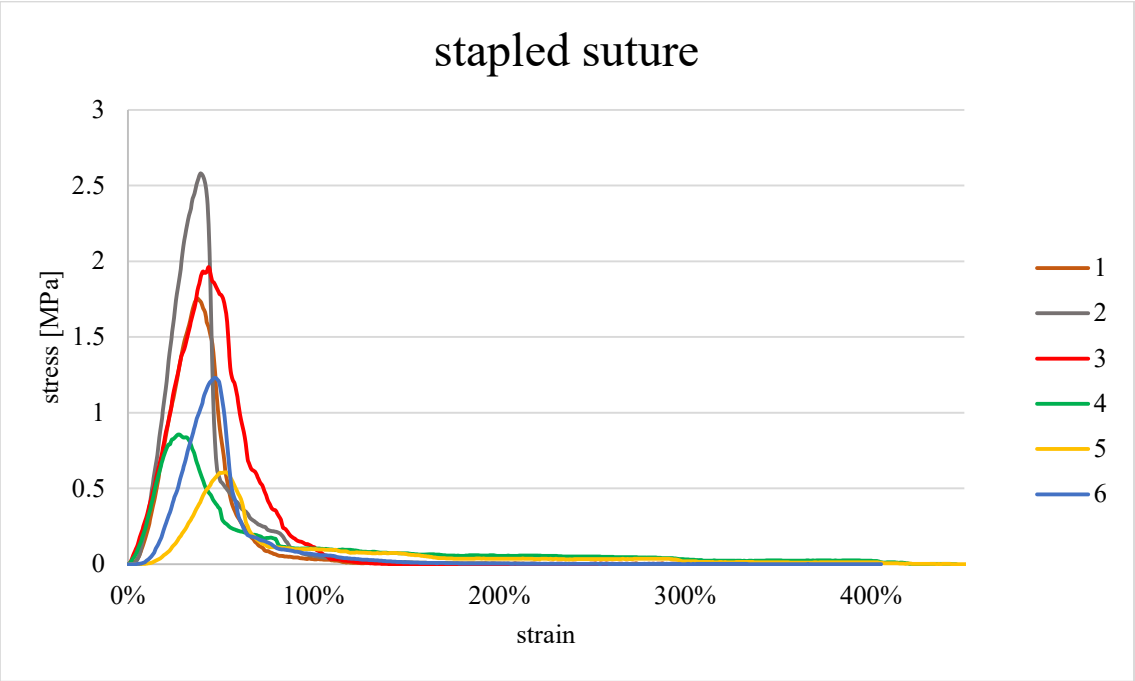

Figure S2 Stress-strain curves obtained with tensile tests on fascia lata patches with stapled suture.The legend shows the name of the samples ("#" in the tables).

Mixed sutures

Table S5 Mechanical properties of two fascia lata patches sutured with staples and the manual suture. One patch has x-oriented fibres and the other y-oriented fibres."t bottom" is the thickness of the patch attached to the bottom grip, "t top" is the thickness of the patch attached to the top grip, "fibres top" and "fibres bottom" are the orientation of the fibres of the bottom and top patch, "failure mode" and "failure area" are the event that led to a decrease of the force recorded and the area in which occurred. To quantify the tensile behaviour of the samples, four properties extracted from the stress-strain curves were considered: the strength (σ_f), the ultimate strain (ε_u), the Young's Modulus (E), and the dissipated specific energy (W) up to the sample complete failure.

#	sample	t bottom	t top	t tot suture	fibres bottom	fibres top	failure mode	failure area	σ_f [MPa]	ε_u [%]	E [MPa]	W [mJ·mm^{-3}]
2	mixed suture	1.39	1.5	2.89	x	y	junction failure	middle/right bottom patch	0.81	232.80	3.39	0.42

Table S6 Mechanical properties of two fascia lata patches sutured with staples and the manual suture. One patch has x-oriented fibres and the other randomly oriented fibres."t bottom" is the thickness of the patch attached to the bottom grip, "t top" is the thickness of the patch attached to the top grip, "fibres top" and "fibres bottom" are the orientation of the fibres of the bottom and top patch, "failure mode" and "failure area" are the event that led to a decrease of the force recorded and the area in which occurred. To quantify the tensile behaviour of the samples, four properties extracted from the stress-strain curves were considered: the strength (σ_f), the ultimate strain (ε_u), the Young's Modulus (E), and the dissipated specific energy (W) up to the sample complete failure.

#	sample	t bottom	t top	t tot suture	fibres bottom	fibres top	failure mode	failure area	σ_f [MPa]	ε_u [%]	E [MPa]	W [mJ·mm^{-3}]
5	mixed suture	0.85	0.77	1.62	x	random	tissue failure	left end top patch	1.11	570.08	3.37	1.05

Table S7 Mechanical properties of two fascia lata patches sutured with staples and the manual suture. The patches have y-oriented fibres."t bottom" is the thickness of the patch attached to the bottom grip, "t top" is the thickness of the patch attached to the top grip, "fibres top" and "fibres bottom" are the orientation of the fibres of the bottom and top patch, "failure mode" and "failure area" are the event that led to a decrease of the force recorded and the area in which occurred. To quantify the tensile behaviour of the samples, four properties extracted from the stress-strain curves were considered: the strength (σ_f), the ultimate strain (ε_u), the Young's Modulus (E), and the dissipated specific energy (W) up to the sample complete failure.

#	sample	t bottom	t top	t tot suture	fibres bottom	fibres top	failure mode	failure area	σ_f [MPa]	ε_u [%]	E [MPa]	W [mJ·mm^{-3}]
1	mixed suture	1.22	0.82	2.04	y	y	junction failure	total top patch	3.41	266.09	7.87	1.65
3	mixed suture	0.96	1.23	2.19	y	y	junction failure	left bottom patch	2.73	312.78	8.56	1.29
4	mixed suture	1.24	0.62	1.86	y	y	junction failure	left end bottom patch	1.90	263.38	4.46	1.10
							mean		**2.68**	**280.75**	**6.96**	**1.35**
							st.dev.		**0.76**	**27.77**	**7.87**	**0.28**

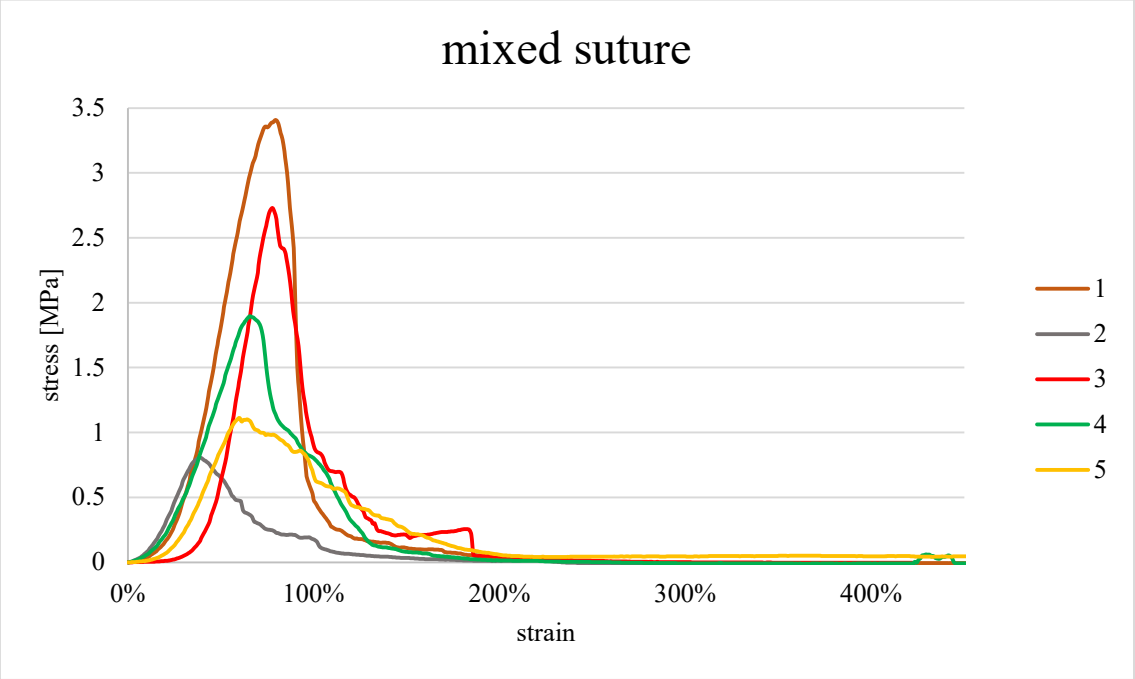

Figure S3 Stress-strain curves obtained with tensile tests on fascia lata patches with the over-sewn stapled (mixed) suture.The legend shows the name of the samples ("#" in the tables).